

Published in final edited form as:

Biomaterials. 2011 February ; 32(5): 1291–1300. doi:10.1016/j.biomaterials.2010.10.018.

Hierarchical and non-hierarchical mineralisation of collagen

Yan Liu¹, Young-Kyung Kim², Lin Dai³, Nan Li⁴, Sara Khan⁵, David H. Pashley⁶, and Franklin R. Tay^{6,7,*}

¹ Department of Stomatology, Tongji Hospital, Tongji Medical College, Huazhong University of Science and Technology, Wuhan, China

² Department of Conservative Dentistry, School of Dentistry, Kyungpook National University, Daegu, Republic of Korea

³ Department of Stomatology, The First Hospital of Wuhan, Wuhan, China

⁴ Department of Osteopedic & Traumatology, University of Traditional Chinese Medicine, Fujian, China

⁵ School of Dentistry, Medical College of Georgia, Augusta, Georgia; USA

⁶ Department of Oral Biology, School of Dentistry, Medical College of Georgia, Augusta, Georgia; USA

⁷ Department of Endodontics, School of Dentistry, Medical College of Georgia, Augusta, Georgia; USA

Abstract

Biom mineralisation of collagen involves functional motifs incorporated in extracellular matrix protein molecules to accomplish the objectives of stabilising amorphous calcium phosphate into nanoprecursors and directing the nucleation and growth of apatite within collagen fibrils. Here we report the use of small inorganic polyphosphate molecules to template hierarchical intrafibrillar apatite assembly in reconstituted collagen in the presence of polyacrylic acid to sequester calcium and phosphate into transient amorphous nanophases. The use of polyphosphate without a sequestration analogue resulted only in randomly-oriented extrafibrillar precipitations along the fibrillar surface. Conversely, the use of polyacrylic acid without a templating analogue resulted only in non-hierarchical intrafibrillar mineralisation with continuous apatite strands instead of discrete crystallites. The ability of using simple non-protein molecules to recapitulate different levels of structural hierarchy in mineralised collagen signifies the ultimate simplicity in Nature's biom mineralisation design principles and challenges the need for using more complex recombinant matrix proteins in bioengineering applications.

1. Introduction

Nature utilises hierarchical structures in intriguing ways to create multifunctional materials. Type I collagen represents an example of Nature's bottom-up approach [1] in self-assembling molecules at the nanoscale to produce highly-ordered macromolecular structures at the microscopical and macroscopical dimensions. For organic-inorganic

*Corresponding author: Franklin R. Tay, Tel.: +1 706 721 3145; fax: +1 706 721 6252, ftay@mail.mcg.edu.

Publisher's Disclaimer: This is a PDF file of an unedited manuscript that has been accepted for publication. As a service to our customers we are providing this early version of the manuscript. The manuscript will undergo copyediting, typesetting, and review of the resulting proof before it is published in its final citable form. Please note that during the production process errors may be discovered which could affect the content, and all legal disclaimers that apply to the journal pertain.

nanocomposites such as bone, this self-assembly process defines the framework and spatial constraints for nucleation and propagation of the reinforcing mineral phase [2]. During initial biomineralisation, no seed crystallites are available within the organic scaffold to serve as nuclei for heterogeneous nucleation [3]. Type I collagen by itself is insufficient to induce nucleation of carbonated apatite from transient amorphous calcium phosphate (ACP) phases [4]. Hence, alternative matrix-mediated mineralisation mechanisms that involve kinetically-driven steps are required to overcome the thermodynamically-unfavourable energy barrier in homogeneous nucleation [3,5]. Noncollagenous matrix macromolecules contribute to these kinetically-driven steps in biomineralisation by stabilising ACPs in the form of nanoprecursors (sequestration motif), and for initiating nucleation and hierarchical assembly of apatite within the collagen scaffold (templating motif) [6–8].

Because of the mineralisation potential of natural noncollagenous matrix proteins, recombinant versions of these molecules or their critical domains are employed in bioengineering [9–11]. Owing to their limited availability and high cost of production, others resort to using polyanionic electrolytes to mimic the functional domains of these proteins. Polycarboxylic acids such as polyacrylic acid or polyaspartic acid are often employed as biomimetic analogues to simulate the sequestration functional motif of matrix proteins [12–15]. When stabilised as ACP nanoparticles, the latter demonstrate mouldable, fluid-like characteristics which enable them to infiltrate the internal water compartments of a collagen fibril [16]. However, the use of only a polycarboxylic acid sequestration analogue results in intrafibrillar mineralisation that lacks the hierarchy of apatite assembly (i.e. overlapping platelets that produce cross-banding patterns) in naturally mineralised collagen [14,15].

Inorganic polyphosphates play important roles in biomineralisation [17,18]. Sodium trimetaphosphate (STMP) is a chemical phosphorylation agent for food proteins [19], carboxymethylcellulose [20] and type I collagen [21]. However, when this simple cyclic polyphosphate molecule is used as a templating analogue without a sequestration agent to stabilise ACP in the form of nanoprecursors, either large extrafibrillar mineral spheres are produced in the vicinity of the collagen fibrils [22] or extrafibrillar apatite crystals are precipitated in a non-oriented manner along the fibrillar surface [23]. Extrafibrillar mineralisation with randomised large crystals deposited over an organic matrix does not reproduce the mechanical properties exhibited by natural mineralised tissues at the nanoscale level [24].

Recent studies on biomimetic collagen mineralisation appear to indicate that both the sequestration and templating functional motifs of matrix proteins involved in biomineralisation have to be reproduced before hierarchical intrafibrillar mineralisation of a collagen matrix can be realised [25,26]. Here we report a polyphosphate-based biomimetic collagen mineralisation strategy using a low molecular weight polyacrylic acid to replicate the sequestration functional motif of the N-terminal fragment of dentine matrix protein-1 (DMP-1) [6], and a small inorganic polyphosphate to replicate the templating functional motif of the C-terminal fragment of DMP-1. Two polyphosphates were employed: sodium trimetaphosphate (STMP) and sodium tripolyphosphate (TPP), a linear tripolyphosphate to demonstrate the temporal and spatial events that lead to the appearance of cross-banding in unstained mineralised collagen. Sodium trimetaphosphate exhibits strong affinity to type I collagen via irreversible binding under alkaline conditions [27]. As TPP may be used directly in lieu of STMP for chemical phosphorylation of food proteins [28], this linear polyphosphate was also investigated to determine its potential for replacing recombinant matrix proteins for hierarchical intrafibrillar apatite assembly within a collagen matrix.

2. Materials and Methods

2.1 Self-assembly of collagen

A single-layer of type I collagen fibrils was reconstituted over formvar-and-carbon-coated 400-mesh Ni TEM grids (Electron Microscopy Sciences, Hatfield, PA, USA) by neutralising a 0.15mg/ml collagen stock solution with ammonia vapour for 4 h [26]. For preparation of collagen stock solution, lyophilised type I collagen powder derived from calf skin (Sigma-Aldrich) was dissolved in 0.1 M acetic acid (pH 3.0) containing phenol red at 4°C overnight. The neutralised collagen solution was left to gel by incubation at 37°C for 3–5 days. To stabilise the structure of the reconstituted collagen fibrils, collagen cross-linking was further performed with 0.3M 1-ethyl-3-(3-dimethylaminopropyl)-carbodiimide (EDC)/0.06M N-hydroxysuccinimide (NHS) (Thermo Scientific Pierce, Rockford IL, USA) for 4 h. Thereafter, the collagen-coated grids were dipped in and out of deionised water and air-dried [26].

2.2 Amorphous calcium phosphate

Composite disks were prepared from a light-polymerisable hydrophilic resin blend containing set white Portland cement powder and silanised silica [26]. Set Portland cement releases calcium hydroxide (pH > 9.25) to facilitate transformation of amorphous calcium phosphate (ACP) to carbonated apatite. The phosphate source was derived from NaN_3 -containing simulated body fluid (SBF): 136.8 mM NaCl, 4.2 mM NaHCO_3 , 3.0 mM KCl, 1.0 mM $\text{K}_2\text{HPO}_4 \cdot 3\text{H}_2\text{O}$, 1.5 mM $\text{MgCl}_2 \cdot 6\text{H}_2\text{O}$, 2.5 mM CaCl_2 , 0.5 mM Na_2SO_4 and 3.08 mM Na_3N . Polyacrylic acid (Mw 1800, Sigma-Aldrich; 1000 $\mu\text{g}/\text{mL}$) was added to SBF to stabilise ACP as nanoprecursors [14,15].

2.3 Collagen mineralisation

Protein phosphorylation with STMP is usually conducted at pH > 11 to hydrolyse and open its closed ring structure [29]. To prevent collagen from denaturing, STMP (Mw 305.9; Sigma-Aldrich) was hydrolysed at pH 12 for 5 h and neutralised to pH 7.4 before use. Four STMP concentrations (wt %) were prepared: 2.5%, 1.25%, 0.625% and 0.313%. TEM grids containing cross-linked collagen ($N = 6$) were immersed in the respective STMP solution for 5 min, rinsed and air-dried. They were floated upside-down over 30 μL of polyacrylic acid-containing SBF placed over a composite disk inside a 100% humidity chamber [26]. Mineralisation was performed initially for 4–24 h to identify the optimal STMP concentration for further mineralisation for 48–72 h. Grids were examined unstained using transmission electron microscopy (JEM-1230, JEOL) and selected area electron diffraction (SAED) at 110 kV. The aforementioned experiments were repeated with TPP ($\text{Na}_5\text{P}_3\text{O}_{10}$, Mw 367.8, Sigma-Aldrich) but omitting the alkaline hydrolysis step.

The collagen negative control (no sequestration and templating analogues) consisted of reconstituted collagen and SBF. The templating analogue control consisted of STMP/TPP-treated collagen and SBF (no sequestration analogue). The sequestration analogue control consisted of reconstituted collagen and polyacrylic acid-containing SBF (no templating analogue).

2.4 Fourier transform–infrared spectroscopy

A Nicolet 6700 FT-IR spectrophotometer (Thermo Scientific, Waltham, MA, USA) with an attenuated total reflection (ATR) setup was used to collect IR spectra from vacuum-dried reconstituted collagen before and after treatment with 2.5 wt% TPP, as well as competitive desorption after treatment with 250 mM NaCl for 24 h. Spectra were collected between 4,000–500 cm^{-1} at 4 cm^{-1} resolution using 32 scans. The data were normalised to the collagen amide I band (1,715–1,596 cm^{-1}) and superimposed for comparison.

3. Results

3.1 Extrafibrillar apatite precipitations

Using a single-layer collagen mineralisation model [26], we confirmed that reconstituted type I collagen does not induce mineralisation in the absence of biomimetic analogues (Supplementary Fig. 1). Only large ACP spherules (*ca.* 1–3 μm) were formed initially at 24 h which were transformed into crystalline patches around the collagen matrix after 48–72 h.

To understand why hierarchical intrafibrillar apatite assembly only occurred when dual biomimetic analogues (i.e. sequestration and templating) were employed, two analogue controls were employed in which one biomimetic analogue was omitted from the mineralisation protocol. For the templating analogue control, no sequestration analog was included in the mineralisation medium. Treatment of reconstituted collagen with 2.5 wt% TPP for 5 min resulted in smaller ACP phases (*ca.* 50–100 nm) in the vicinity of the collagen fibrils after 24 h. These ACP phases were also attached to various extents on the fibrillar surface (Fig. 1a, b). They were transformed into blunted, finger-like immature apatite after 48 h (Fig. 1c), and further into needle-shaped apatite that were randomly precipitated over the surface of collagen fibrils after 72 h (Fig. 1d). No intrafibrillar mineralisation could be observed. Despite the absence of a sequestration analogue, ACP phases were smaller than those in the collagen negative control.

3.2 Non-hierarchical intrafibrillar mineralisation

In the sequestration analogue control, 1000 mg/mL polyacrylic acid was included in the mineralisation medium but did not treat the reconstituted collagen with STMP or TPP. Two ACP phases were formed after 4 h (Supplementary Fig. 2). The relatively larger ACP phase were 50–100 nm in diameter and the smaller ACP nanophase was less than 10 nm in diameter. Only the smaller ACP nanophases were useful for intrafibrillar mineralisation (shown later). After 24 h, collagen fibrils appeared swollen and were infiltrated by a highly electron-dense amorphous mineral phase (Fig. 2a). The ACP nanophases that were present in the vicinity of unmineralised fibrils were predominantly absent from the surface of those swollen, smooth, electron-dense fibrils (Fig. 2b). After 72 h, the swollen appearance of the fibrils disappeared and the coalesced ACP was transformed into fibrous intrafibrillar mineral strands that lacked cross-banding patterns (Fig. 2c). Mineralised strands within those fibrils appeared to be continuous at high magnification (Fig. 2d).

3.3 Hierarchical intrafibrillar mineralisation

Figures 3 and 4 represent the temporal and spatial events associated with the use of different templating analogue concentrations (0.313–2.5 wt%) for collagen mineralisation in the presence of 1000 $\mu\text{g}/\text{mL}$ polyacrylic acid as the sequestration analogue. As similar results were obtained for STMP and TPP, only one polyphosphate templating analogue is illustrated for the early amorphous (STMP; 4–12 h) and crystalline (TPP, 48–72 h) stages of intrafibrillar mineralisation. In the amorphous stage (Fig. 3), less and less ACP nanophases aggregated along the fibrillar surface with increasing STMP concentrations, while increasingly apparent cross-banding corresponding to the D-spacing of collagen molecules could be seen within the fibrils. Despite the appearance of cross-banding, SAED indicated that intrafibrillar minerals were amorphous at this stage (not shown). In the crystalline stage (Fig. 4), progressively noticeable hierarchical apatite assembly could be identified with increasing TPP concentrations. This ranged from the occurrence of continuous microfibrillar strands without cross-banding at 0.313 wt%, to the appearance of vague cross-banding at 0.625 wt%, to distinct cross-banding at 1.25 wt% and 2.5 wt% TPP. With 2.5% TPP, collagen fibrils with cross-banding patterns produced by discrete apatite crystallites could be identified only from partially-mineralised collagen fibrils; the completely-mineralised fibrils

were too electron-dense for cross-banding to be observed without resorting ultramicrotomy of epoxy resin-embedded specimens.

Figure 5 depicts the spatial and temporal events associated with the use of the optimal TPP concentration (2.5 wt%) for collagen mineralisation in the presence of polyacrylic acid. At the late amorphous stage (24 h), electron-dense swollen fibrils could be identified (Fig. 5a). Unlike those swollen collagen previously shown in the sequestration analogue control, the use of dual biomimetic analogues resulted in highly regular cross-banding within the swollen fibrils. At the crystalline stage (47–72 h), most of the collagen fibrils were heavily mineralised (Fig. 5b) and cross-banding could only be discerned from partially-mineralised fibrils (Fig. 5c). The presence of intrafibrillar apatite crystallites also protected collagen fibrils from dehydration shrinkage (Fig. 5c). Apatite nanoplatelets were 25–40 nm long along their C-axis and were responsible for the cross-banded appearance of the unstained mineralised fibrils (Fig. 5d). Similar results could be identified from the STMP specimens (Supplementary Fig. 3) although collagen mineralisation was more labour and technique-sensitive. Arc-shaped patterns were present when electron diffraction was performed directly over non-overlapped mineralised fibrils. Conversely, only continuous rings were identified when electron diffraction was performed over overlapped mineralized fibrils (Supplementary Fig. 4).

3.4 Fourier transform–infrared spectroscopy

Infrared spectra of the fingerprint region of collagen between 1800–700 cm^{-1} are shown in Fig. 6. Before TPP treatment, type I collagen demonstrated characteristic Amide I, II and III bands at ≈ 1630 , 1540 and 1230 cm^{-1} , respectively. After TPP treatment, new phosphate peaks could be identified at ≈ 1110 , 974 and 887 cm^{-1} that are attributed to vibrations in the ν_3 asymmetric and ν_1 symmetric stretching modes of the phosphate groups [30]. There was also a simultaneous reduction in the series of collagen bands between Amide II and III that are assigned to wagging vibrations from the glycine backbone and proline side chains [31]. After 24 h of competitive desorption with 250 mM NaCl, the new phosphate peaks disappeared and the spectrum was similar to that of the original collagen.

4. Discussion

The contribution of transient ACP phases to the development of vertebrate mineralised tissues has been supported by recent studies reporting that such a strategy is involved in the formation of bone [32] and teeth [33]. Although ACPs may be synthesised inorganically at the microscopical length scale using different chemical systems [34], a size exclusion mechanism limits the dimension of ACP phases that can penetrate the internal water compartments of a collagen fibril [35]. Molecules larger than 40 kDa are completely excluded from these internal water compartments, while molecules smaller than 6 kDa can diffuse into all the water compartments within the collagen fibril. Thus, it is logical to assume that ACP nanophases have to be smaller than 40 kDa in order for them to penetrate and displace water from at least some internal compartments of a collagen fibril. This explains why the relatively larger ACP phases shown in Fig. 1 and Supplementary Figure 2 are incapable of participating in intrafibrillar mineralisation. One of the functional motifs of matrix proteins involved in biomineralisation is to act as a sequestration agent for stabilising ACP in the form of nanophases [36]. Dentin matrix protein-1, an acidic matrix protein, is cleaved into a larger N-terminal and a smaller C-terminal fragment. The aspartic acid-rich N-terminal segment helps stabilise ACP into nanoparticles [6]. A similar ACP stabilisation motif was also observed for a 20-kD cleavage product of amelogenin [37]. Thus, a sequestration biomimetic analogue is required to simulate the function of these natural protein molecules.

Sodium tripolyphosphate has been used as an anionic surfactant to inhibit crystal growth in the synthesis of calcite nanocrystals [38]. Similar to STMP [27], a small amount of the collagen-bound TPP could have been displaced by anions derived from the mineralisation medium, resulting in the small ACP phases in the vicinity of the collagen fibrils. The remaining collagen-bound TPP caused ACP phases to be attached directly to the fibrillar surface, which assumed different shapes (Fig. 1a) due to their initial mouldable characteristics [16]. Exclusive extrafibrillar precipitations identified from this control parallels the results achieved when STMP was used for mineralising collagen without a sequestration analogue [15]. Taken together, these results indicate that polyphosphates such as STMP or TPP alone produces ACP phases that are too large to penetrate the internal water compartments of fibrillar collagen and hence intrafibrillar mineralisation does not occur.

As demonstrated in Figs. 2 and 4a, the use of a sequestration analogue alone or in combination with insufficient templating analogue does not result in the type of intrafibrillar mineralisation that resembles what has been perfected by Nature. During the initial mineralisation stage, it appears that the lateral spacings between collagen molecules can be expanded temporarily to accommodate the infiltrated ACP nanophases. The reason for this swelling is unknown. A possible explanation is that ACP contains more water than apatite within its intercluster spaces [34,39]. Thus, a larger volume of ACP is required if apatite has to fully replace the original volume occupied by water within a collagen fibril. During transformation of ACP into more compactly-packed apatite, water is displaced from the internal water compartments of the collagen fibril, resulting in progressive dehydration of the fibril [13]. This provides a mechanism for the swollen fibril to return to its original dimension.

In Fig. 2d, we observed that the mineralised fibrous strands appeared to be continuous instead of existing as discrete crystallites. Although the results from the sequestration analogue control support previous studies that intrafibrillar mineralisation occurs with the use of a templating analogue alone [14,15], the non-hierarchical mineralisation observed appears to suggest that the mineralisation mechanism involved is considerably different from that utilised by natural matrix proteins in biomineralisation of vertebrate collagenous tissues. In the absence of a templating analogue to direct the nucleation of discrete apatite nanocrystals, we suggest that the interconnecting water-filled volume within the collagen fibril may be crystallised as a continuum and moulded into a single crystalline structure. Such a crystallisation mechanism produces unusual mineralised collagen entities that resemble the monolithic single-crystal structure in sea urchin spines [40] or siliceous bioskeletons [41], albeit within the nanoscale internal environment of a collagen fibril. In this polymer-induced liquid precursor [16] or polymer-assisted moulding process [42], single crystals without definitive crystalline planes may be created that bend around curvatures and contain porosities. Although this mineralisation mechanism is important in amorphous calcium carbonate and amorphous silica-based biomineralisation systems, formation of a single crystal with curvature and fenestrations is not what Nature has intended apatite to be deposited within collagen fibrils in vertebrates to achieve their load bearing function [24].

For the collagen that were mineralised in the presence of both the sequestration and the templating analogues, visualisation of cross-banding in only incompletely-mineralised fibrils is analogous to etching naturally mineralised collagen with mild acids to enable collagen cross-banding patterns to be identified with atomic force microscopy [43]. This hierarchical arrangement is identical to that observed in naturally mineralised type I collagen [2]. Matrix phosphoproteins serve as templates for apatite nucleation and growth within the gap zones of collagen fibrils [44]. When bound to collagen, these highly-phosphorylated polyanionic

macromolecules function as templates [45] by attracting calcium ions and induce apatite nucleation within the gap zones of the collagen fibril. During this process, the comparative loose amorphous structure in ACPs is transformed into a more closely-packed crystalline structure [46]. The phosphoserine-rich C-terminal fraction of cleaved DMP-1 is thought to be responsible for apatite nucleation [6]. Phosphophoryn is another important initiator and modulator for apatite growth due to its excellent binding capacity for calcium ions as well as its strong affinity to collagen [47]. Bone sialoprotein is another acidic phosphoprotein which is capable of binding to collagen and nucleating apatite [48]. The polyphosphate analogues appear to replicate the templating function of these phosphoproteins well enough for hierarchical apatite assembly to be discerned within the biomimetically-mineralised collagen fibrils. Together with the controls, these results highlight the complementary contribution of the two functional motifs of matrix proteins involved in biomineralisation of collagen; failure to replicate either functional motif will result in exclusive extrafibrillar precipitations or non-hierarchical intrafibrillar mineralisation of a collagen matrix (Figure 7).

It has been shown that STMP can bind irreversibly to collagen by forming new covalent bonds [22,23], We were also able to observe formation of new phosphate peaks when Fourier transform-infrared spectroscopy was used to examine the interaction between TPP and reconstituted collagen (Fig. 6). However, these new phosphate peaks disappeared after the TPP-doped collagen was immersed for 24 h in 250 mM NaCl, indicating that the cross-linking is reversible and non-covalent in nature. As TPP forms ionic cross-links (ionic bridges) between chitosan molecules via interacting with their amine groups [49], similar ionic bridges may be formed when TPP interacts with collagen molecules. Although ionic cross-linking not as stable as covalent cross-linking, this cross-linking procedure is an important textile treatment process that increases the crease resistance of fabrics [50]. There are five negatively charged ionisable groups in TPP with different pKa values (pKa1=1, pKa2=2, pKa3=2.79, pKa4=6.47, pKa5=9.24) [51]. A 2.5 wt% TPP solution has a pH value of 8.5 with at least four ionisable OH⁻ groups. Thus, TPP may form ionic cross-links with collagen as a reversible binding mechanism, with the remaining free OH⁻ groups contributing to the attraction of ACP nanophases. Ionic cross-linking provides the rationale for displacement of collagen-bound TPPs to form relatively large ACP phases even in the absence of polyacrylic acid (Fig. 1b). Figure 8 illustrates the possible mechanism that may be involved in the binding of TPP to collagen.

5. Conclusions

We demonstrate here a highly hierarchical assembly of intrafibrillar apatite crystallites in reconstituted collagen mineralised *ex-situ* with biomimetic analogues of extracellular matrix proteins. From a developmental biology perspective, the results of this work provide important confirmation of the two distinct but complementary functional motifs in matrix proteins involved in vertebrate collagen mineralisation. It is possible that a single sequestration functional motif is probably what is required for biomineralisation of invertebrate systems that involve fusion of amorphous mineral precursor phases into porous single crystalline structures. The creativity of evolution in which nature timelessly explores all options and finds the best solution is surprisingly instructive. The notions that these functional motifs are highly conserved in matrix proteins from different animal species and that they can be replicated using small, non-protein molecules imply that the biomineralization principles perfected by Nature are, ultimately, simplistic and clear-cut in design. The complexity of different proteins involved in the process probably represents the means by which the proteins incorporating these functional motifs are produced within the intracellular milieu and delivered to the external environment. One of the main challenges of biomimetics is that it demands creative solutions. Nature's store of ideas is valuable only if it can be translated into usable technology. This study demonstrates that small non-protein

biomimetic molecules may be substituted for complex recombinant matrix proteins or their functional domains for applications that involve the use of mineralized collagen. The latter may include porous, three-dimensional mineralised collagen scaffolds to enhance stem cell proliferation and coating of orthopaedic implants with collagen pre-impregnated with hierarchical intrafibrillar nanoapatite.

Supplementary Material

Refer to Web version on PubMed Central for supplementary material.

Acknowledgments

This work was supported by grant R21 DE019213 from NIDCR (PI. Franklin Tay). We thank Michelle Barnes for secretarial support, Robert Smith for TEM assistance.

References

1. Wong TS, Brough B, Ho CM. Creation of functional micro/nano systems through top-down and bottom-up approaches. *Mol Cell Biomech* 2009;6:1–55. [PubMed: 19382535]
2. Traub W, Arad T, Weiner S. Three-dimensional ordered distribution of crystals in turkey tendon collagen fibers. *Proc Natl Acad Sci USA* 1989;86:9822–9826. [PubMed: 2602376]
3. Wang L, Nancollas GH. Pathways to biomineralization and biodemineralization of calcium phosphates: the thermodynamic and kinetic controls. *Dalton Trans* 2009;15:2665–2672. [PubMed: 19333487]
4. Saito T, Arsenault AL, Yamauchi M, Kuboki Y, Crenshaw MA. Mineral induction by immobilized phosphoproteins. *Bone* 1997;21:305–311. [PubMed: 9315333]
5. Cölfen H. Bio-inspired mineralization using hydrophilic polymers. *Top Curr Chem (Springer-Verlag, Berlin: Heidelberg)* 2007;271:1–77.
6. Gajjeraman S, Narayanan K, Hao J, Qin C, George A. Matrix macromolecules in hard tissues control the nucleation and hierarchical assembly of hydroxyapatite. *J Biol Chem* 2007;282:1193–1204. [PubMed: 17052984]
7. Weiner S. Biomineralization: a structural perspective. *J Struct Biol* 2008;163:229–234. [PubMed: 18359639]
8. Hao J, Ramachandran A, George A. Temporal and spatial localization of the dentin matrix proteins during dentin biomineralization. *J Histochem Cytochem* 2009;57:227–237. [PubMed: 19001636]
9. Sfeir, C.; Cambell, P.; Jadlowiex, JA.; Kumta, P. Method of inducing biomineralization method of inducing bone regeneration and methods related thereof. US Patent Appl. 20070087959. 2007.
10. Kaplan, DL.; Huang, J.; Wong, CPF.; Naik, R.; George, A. Fibrous protein fusions and use thereof in the formation of advanced organic/inorganic composite materials. US Patent Appl. 20080293919. 2008.
11. Goldberg, HA.; Hunter, GK.; Tye, CE. Bone sialoprotein collagen-binding peptides. US Patent Appl. 20090005298. 2009.
12. Girija EK, Yokogawa Y, Nagata F. Apatite formation on collagen fibrils in the presence of polyacrylic acid. *J Mater Sci Mater Med* 2004;15:593–599. [PubMed: 15386967]
13. Chesnick IE, Mason JT, Giuseppetti AA, Eidelman N, Potter K. Magnetic resonance microscopy of collagen mineralization. *Biophys J* 2008;95:2017–2026. [PubMed: 18487295]
14. Deshpande AS, Beniash E. Bio-inspired synthesis of mineralized collagen fibrils. *Cryst Growth Des* 2008;8:3084–3090.
15. Jee SS, Thula TT, Gower LB. Development of bone-like composites via the polymer-induced liquid-precursor (PILP) process. Part I: influence of polymer molecular weight. *Acta Biomater* 2010;6:3676–3686. [PubMed: 20359554]
16. Gower LB. Biomimetic model systems for investigating the amorphous precursor pathway and its role in biomineralization. *Chem Rev* 2008;108:4551–4627. [PubMed: 19006398]

17. Omelon SJ, Grynblas MD. Relationships between polyphosphate chemistry, biochemistry and apatite biomineralization. *Chem Rev* 2008;108:4694–4715. [PubMed: 18975924]
18. Usui Y, Uematsu T, Uchihashi T, Takahashi M, Takahashi M, Ishizuka M, et al. Inorganic polyphosphate induces osteoblastic differentiation. *J Dent Res* 2010;89:504–509. [PubMed: 20332330]
19. Li Y, de Vries R, Slaghek T, Timmermans J, Cohen Stuart MA, Norde W. Preparation and characterization of oxidized starch polymer microgels for encapsulation and controlled release of functional ingredients. *Biomacromolecules* 2009;10:1931–1938.
20. Leone G, Torricelli P, Giardino R, Barbucci R. New phosphorylated derivatives of carboxymethylcellulose with osteogenic activity. *Polym Adv Technol* 2008;19:824–830.
21. Gunasekaran, S. Purifying type I collagen using two papain treatments and reducing and delipidation agents. US Patent Office. 6548077. 2003.
22. Li X, Chang J. Preparation of bone-like apatite-collagen nanocomposites by a biomimetic process with phosphorylated collagen. *J Biomed Mater Res A* 2008;85:293–300. [PubMed: 17688292]
23. Xu Z, Neoh KG, Kishen A. A biomimetic strategy to form calcium phosphate crystals on type I collagen substrate. *Mat Sci Eng C* 2010;30:822–826.
24. Gupta HS, Seto J, Wagermaier W, Zaslansky P, Boesecke P, Fratzl P. Cooperative deformation of mineral and collagen in bone at the nanoscale. *Proc Natl Acad Sci USA* 2006;103:17741–17746. [PubMed: 17095608]
25. Tay FR, Pashley DH. Guided tissue remineralisation of partially demineralised human dentine. *Biomaterials* 2008;29:1127–1137. [PubMed: 18022228]
26. Kim YK, Gu LS, Bryan TE, Kim JR, Chen L, Liu Y, et al. Mineralization of reconstituted collagen using polyvinylphosphonic acid/polyacrylic acid templating matrix protein analogues in the presence of calcium, phosphate and hydroxyl ions. *Biomaterials* 2010;31:6618–6627. [PubMed: 20621767]
27. Gu LS, Kim J, Kim YK, Liu Y, Dickens SH, Pashley DH, et al. A chemical phosphorylation-inspired design for Type I collagen biomimetic remineralization. *Dent Mater*. 2010 [Epub ahead of print].
28. Zhang K, Li Y, Ren Y. Research on the phosphorylation of soy protein isolate with sodium tripolyphosphate. *J Food Eng* 2007;79:1233–1237.
29. Shen CY. Alkaline hydrolysis of sodium trimetaphosphate in concentrated solutions and its role in built detergents. *Ind Eng Chem Prod Res Dev* 1966;5:272–276.
30. Arai Y, Sparks DL. ATR-FTIR spectroscopic investigation on phosphate adsorption mechanisms at the ferrihydrite-water interface. *J Colloid Interface Sci* 2001;241:317–326.
31. Jackson M, Choo L-P, Watson PH, Halliday WC, Mantsch HH. Beware of connective tissue proteins: assignment and implications of collagen absorptions in infrared spectra of human tissues. *Biochim Biophys Acta* 1995;1270:1–6.
32. Mahamid J, Sharir A, Addadi L, Weiner S. Amorphous calcium phosphate is a major component of the forming fin bones of zebrafish: Indications for an amorphous precursor phase. *Proc Natl Acad Sci USA* 2008;105:12748–12753. [PubMed: 18753619]
33. Deshpande AS, Fang PA, Simmer JP, Margolis HC, Beniash E. Amelogenin-collagen interactions regulate calcium phosphate mineralization in vitro. *J Biol Chem* 2010;295:19277–19287. [PubMed: 20404336]
34. Combes C, Rey C. Amorphous calcium phosphates: synthesis, properties and uses in biomaterials. *Acta Biomater* 2010;6:3362–3378. [PubMed: 20167295]
35. Toroian D, Lim JE, Price PA. The size exclusion characteristics of type I collagen: implications for the role of noncollagenous bone constituents in mineralization. *J Biol Chem* 2007;282:22437–22447. [PubMed: 17562713]
36. He G, Gajjeraman S, Schultz D, Cookson D, Qin C, Butler WT, et al. Spatially and temporally controlled biomineralization is facilitated by interaction between self-assembled dentin matrix protein 1 and calcium phosphate nuclei in solution. *Biochemistry* 2005;44:16140–16148. [PubMed: 16331974]

37. Kwak SY, Wiedemann-Bidlack FB, Beniash E, Yamakoshi Y, Simmer JP, Litman A, et al. Role of 20-kDa amelogenin (P148) phosphorylation in calcium phosphate formation in vitro. *J Biol Chem* 2009;284:18972–18979. [PubMed: 19443653]
38. Sonawane SH, Gumfekar SP, Meshram S, Deosarkar MP, Mahajan CM, Khanna P. Combined effect of surfactant and ultrasound on nano calcium carbonate synthesized by crystallization process. *Int J Chem React Eng* 2009;7:A47.
39. Sedlak JM, Beebe RA. Temperature programmed dehydration of amorphous calcium phosphate. *J Colloid Interface Sci* 1974;47:483–489.
40. Müller WE, Wang X, Cui FZ, Jochum KP, Tremel W, Bill J, et al. Sponge spicules as blueprints for the biofabrication of inorganic-organic composites and biomaterials. *Appl Microbiol Biotechnol* 2009;83:397–413. [PubMed: 19430775]
41. Cölfen H. Single crystals with complex form via amorphous precursors. *Angew Chem Int Ed Engl* 2008;47:2351–2353. [PubMed: 18306202]
42. Meldrum FC, Ludwigs S. Template-directed control of crystal morphologies. *Macromol Biosci* 2007;7:152–62. [PubMed: 17295402]
43. Balooch M, Habelitz S, Kinney JH, Marshall SJ, Marshall GW. Mechanical properties of mineralized collagen fibrils as influenced by demineralization. *J Struct Biol* 2008;162:404–410. [PubMed: 18467127]
44. George A, Veis A. Phosphorylated proteins and control over apatite nucleation, crystal growth, and inhibition. *Chem Rev* 2008;108:4670–4693. [PubMed: 18831570]
45. Zhang TH, Liu XY. How does a transient amorphous precursor template crystallization. *J Am Chem Soc* 2007;129:13520–13526. [PubMed: 17929918]
46. Tsuji T, Onuma K, Yamamoto A, Iijima M, Shiba K. Direct transformation from amorphous to crystalline calcium phosphate facilitated by motif-programmed artificial proteins. *Proc Natl Acad Sci USA* 2008;105:16866–16870. [PubMed: 18957547]
47. He G, Ramachandran A, Dahl T, George S, Schultz D, Cookson D, et al. Phosphorylation of phosphophoryn is crucial for its function as a mediator of biomineralization. *J Biol Chem* 2005;280:33109–33114. [PubMed: 16046405]
48. Baht GS, O'Young J, Borovina A, Chen H, Tye CE, Karttunen M, et al. Phosphorylation of Ser136 is critical for potent bone sialoprotein-mediated nucleation of hydroxyapatite crystals. *Biochem J* 2010;428:385–395. [PubMed: 20377527]
49. Hu M, Li Y, Decker EA, Xiao H, McClements DC. Influence of tripolyphosphate cross-linking on the physical stability and lipase digestibility of chitosan-coated lipid droplets. *J Agric Food Chem* 2010;58:1283–1289. [PubMed: 19921835]
50. Hauser PJ, Smith CB, Hashem MM. Ionic crosslinking of cotton. *Autex Res J* 2004;4:95–100.
51. Shu XZ, Zhu KJ. The influence of multivalent phosphate structure on the properties of ionically cross-linked chitosan films for controlled drug release. *Eur J Pharm Biopharm* 2002;54:235–243. [PubMed: 12191697]

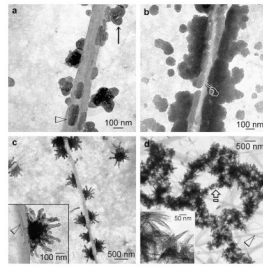


Figure 1.

Unstained TEM showing only extrafibrillar mineralisation in the templating analogue control (no sequestration analogue in mineralisation medium). **(a)** After 24 hours, partially-coalesced ACPs (arrow) were attached to the fibril surface (open arrowhead) but were too large to penetrate the collagen fibril. **(b)** An unmineralised collagen fibril (pointer) with heavier ACP surface aggregation. **(c)** Some ACP phases were transformed into immature finger-like immature apatite (inset). **(d)** After 72 hours, spherules of needle-shaped apatite crystallites (inset; > 100 nm long) coated the surface (open arrowhead) of unmineralised collagen fibrils (open arrowhead).

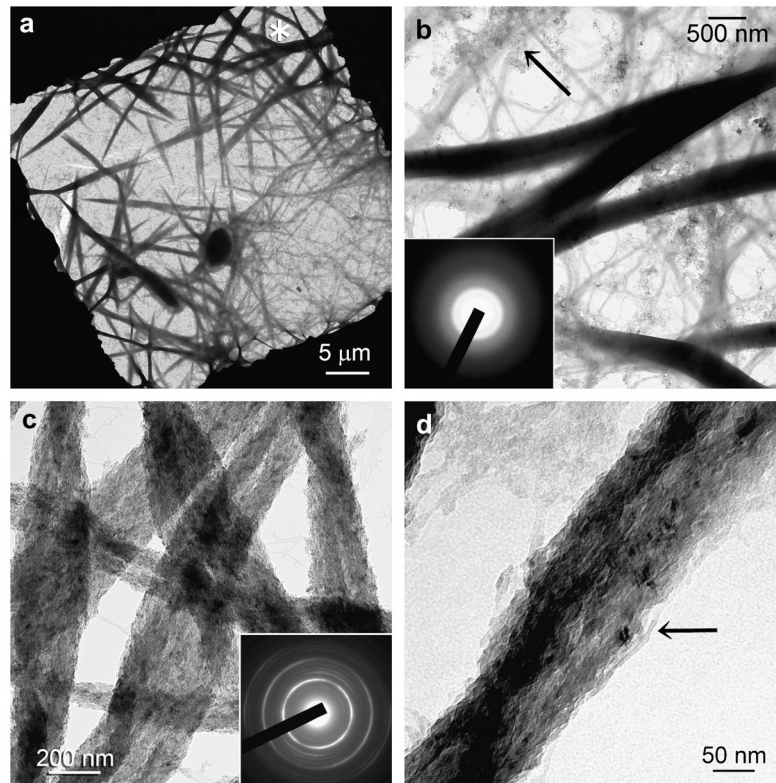


Figure 2. Unstained TEM showing the temporal events associated with non-hierarchical intrafibrillar mineralisation in the sequestration analogue control (no templating analogue). **(a)** Grid space showing swollen electron-dense collagen fibrils (asterisk) after 24 hours. **(b)** Swollen, electron-dense fibrils with a smooth appearance. ACP nanoparticle clusters were seen predominantly around unmineralised fibrils (arrow). ACP nanoparticles appeared to have penetrated the swollen fibrils and coalesced into a continuous amorphous mineral phase (inset). **(c)** After 72 h of mineralization, collagen fibrils were no longer swollen and exhibited a fibrous appearance. Although they contained intrafibrillar mineral, they lacked cross-banding patterns. Inset: Selected area electron diffraction (SAED) of individual mineralised fibrils produced ring patterns that are characteristic of apatite (note arc-shaped patterns indicating that minerals are arranged along the longitudinal axis of the collagen fibrils – see also Supplementary Fig.4). **(d)** High magnification of a mineralised fibril showing the continuity of the mineral strands and absence of discrete crystallites (arrow).

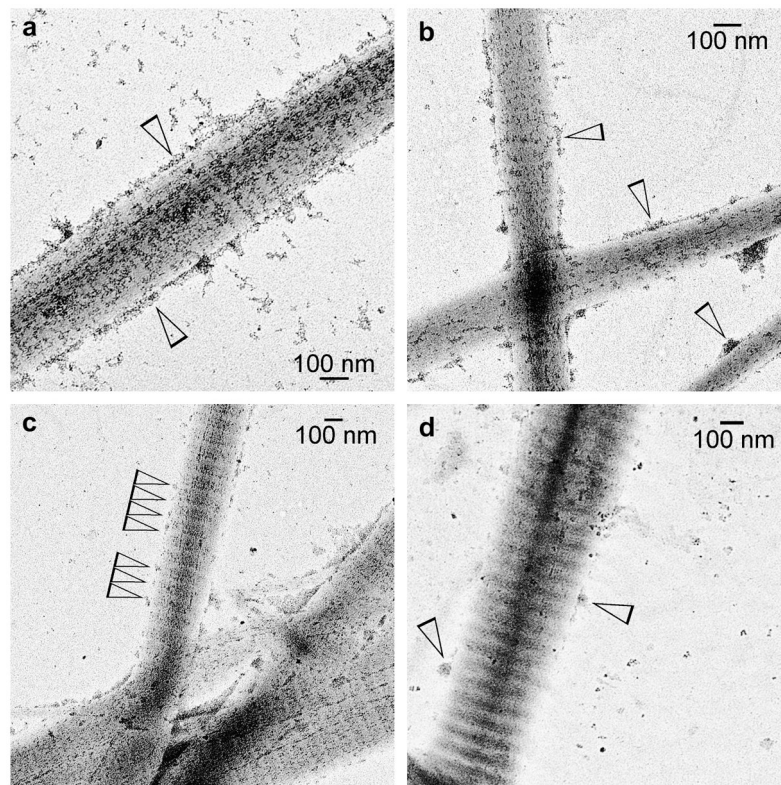


Figure 3. Unstained TEM showing the spatial effects of different templating analogue concentrations on the amorphous stage of hierarchical intrafibrillar mineralisation in the presence of a sequestration analogue. Sodium trimetaphosphate **(a)** 0.313 wt%, **(b)** 0.625 wt%, **(c)** 1.25 wt %, **(d)** 2.5 wt% was used as the example. Only ACP nanoparticle aggregates were identified along the collagen fibril surfaces (open arrowheads). Large ACP phases (see Supplementary Figure 2) were not involved in intrafibrillar mineralisation.

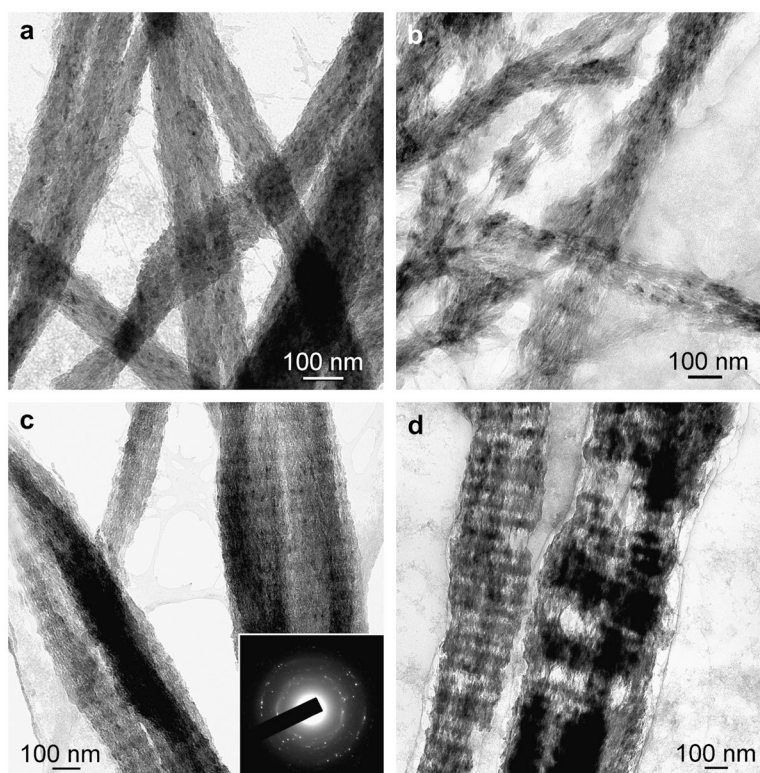


Figure 4. Unstained TEM showing the spatial effects of different templating analogue concentrations on the crystalline stage of hierarchical intrafibrillar mineralisation in the presence of a sequestration analogue. Sodium triphosphate (**(a)** 0.313%, **(b)** 0.625%, **(c)** 1.25%, **(d)** 2.5% was used as the example. The similarity between Fig. 4(a) and Fig. 2(c) suggests that 0.313 wt% sodium triphosphate is insufficient to produce hierarchical intrafibrillar banding. Inset in (c) indicates crystalline phase that is characteristic of apatite and is applicable to all subfigures. Partially-mineralised collagen fibrils were illustrated as the heavily-mineralised fibrils were too electron-dense for cross-banding to be discerned in bulk, unsectioned fibrils.

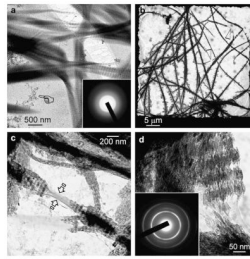


Figure 5.

Unstained TEM of collagen treated with 2.5 wt% sodium tripolyphosphate and mineralised in polyacrylic acid-containing SBF. **(A)** Swollen, cross-banded collagen fibrils containing amorphous electron-dense minerals (inset) after 24 h. **(B)** Grid space showing heavy mineralisation of the collagen fibrils after 72 h. A few fibrils contained unmineralised regions (open arrowheads). **(C)** Partially-mineralised collagen fibril with cross-banding created by intrafibrillar mineral assembly. Absence of minerals in the unmineralised region (between open arrows) resulted in extensive shrinkage during chemical dehydration for TEM. **(D)** Partially-mineralised collagen fibril showing hierarchical arrangement of overlapping nanoplatelets. Inset: SAED with ring patterns corresponding to those of poorly-crystalline apatite (note: arc-shaped patterns indicating that minerals are arranged along the longitudinal axis of the collagen fibrils – see also Supplementary Fig.4).

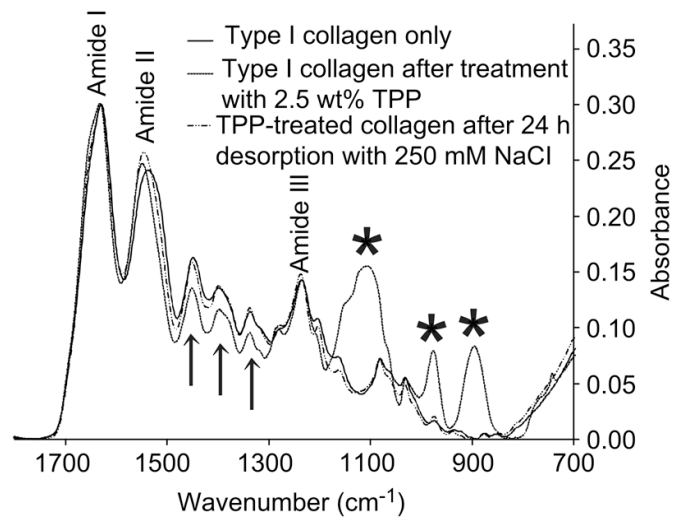


Figure 6. Infrared spectra (1800–700 cm^{-1}) of type I collagen before and after treatment with 2.5 wt% sodium triphosphate and after subjected to competitive desorption with 250 mM NaCl for 24 h. After triphosphate treatment, new phosphate peaks could be identified (asterisks). There was also a simultaneous reduction in the series of collagen bands between Amide II and III (arrows). After 24 h of NaCl desorption, the spectrum was similar to that of the original type I collagen. This suggests that the sodium polyphosphate binding mechanism is exclusively electrostatic in nature, probably via the formation of ionic bridges.

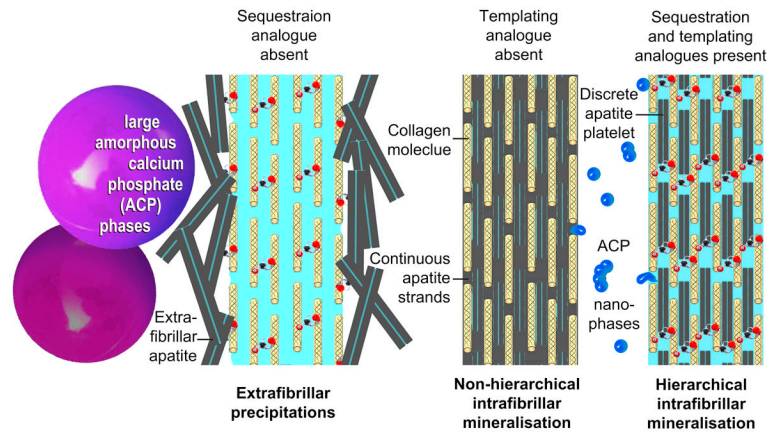


Figure 7. Schematic showing the different status of apatite deposition around and within a collagen fibril in the presence of different combinations of sequestration and templating analogues.

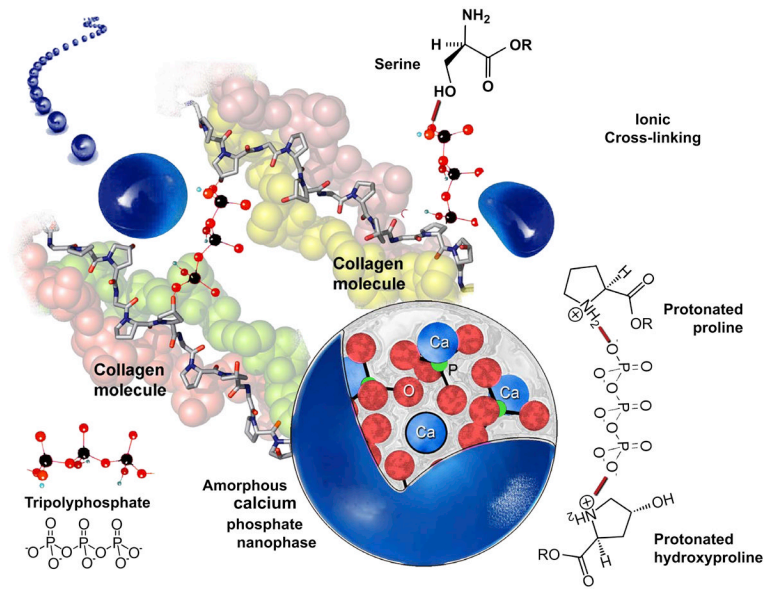


Figure 8. Schematic depicting possible ionic cross-linking involved with binding of sodium triphosphate anions to collagen molecules. Free hydroxyl ions that do not interact with collagen molecules contribute to recruitment of polyacrylic acid-stabilised amorphous calcium phosphate nanophase and induction of apatite nucleation.